Available online at www.sciencedirect.com
SCIENCE DIRECT®
Journal of volcanology and geothermal research
ELSEVIER
Journal of Volcanology and Geothermal Research 150 (2006) 313–327
www.elsevier.com/locate/jvolgeores

Vertical deformation monitoring at Axial Seamount since its 1998 eruption using deep-sea pressure sensors

William W. Chadwick Jr. [a,*], Scott L. Nooner [b], Mark A. Zumberge [b], Robert W. Embley [c], Christopher G. Fox [d]

[a] *Oregon State University/NOAA, 2115 SE OSU Drive, Newport, OR 97365, USA*
[b] *Institute of Geophysics and Planetary Physics, Scripps Institution of Oceanography, La Jolla, CA 92093, USA*
[c] *NOAA/Pacific Marine Environmental Laboratory, Newport, OR 97365, USA*
[d] *NOAA/National Geophysical Data Center, Boulder, CO 80305, USA*

Received 25 May 2004; received in revised form 15 November 2004
Available online 16 August 2005

Abstract

Pressure measurements made on the seafloor at depths between 1500 and 1700 m at Axial Seamount, an active submarine volcano on the Juan de Fuca Ridge in the northeast Pacific Ocean, show evidence that it has been inflating since its 1998 eruption. Data from continuously recording bottom pressure sensors at the center of Axial's caldera suggest that the rate of inflation was highest in the months right after the eruption (20 cm/month) and has since declined to a steady rate of ~15 cm/year. Independent campaign-style pressure measurements made each year since 2000 at an array of seafloor benchmarks with a mobile pressure recorder mounted on a remotely operated vehicle also indicate uplift is occurring in the caldera at a rate up to 22 ± 1.3 cm/year relative to a point outside the caldera. The repeatability of the campaign-style pressure measurements progressively improved each year from ± 15 cm in 2000 to ± 0.9 cm in 2004, as errors were eliminated and the technique was refined. Assuming that the uplift has been continuous since the 1998 eruption, these observations suggest that the center of the caldera has re-inflated about 1.5 ± 0.1 m, thus recovering almost 50% of the 3.2 m of subsidence that was measured during the 1998 eruption. This rate of inflation can be used to calculate a magma supply rate of 14×10^6 m^3/year. If this rate of inflation continues, it also suggests a recurrence interval of ~16 years between eruptions at Axial, assuming that it will be ready to erupt again when it has re-inflated to 1998 levels.

Keywords: volcano inflation; ground deformation monitoring; seafloor geodesy; bottom pressure recorder

1. Introduction

The purpose of vertical deformation monitoring at active volcanoes is to detect the effects of underground magma movements and provide information

* Corresponding author. Tel.: +1 541 867 0179; fax: +1 541 867 3907.
E-mail address: bill.chadwick@noaa.gov (W.W. Chadwick).

0377-0273/$ - see front matter © 2005 Elsevier B.V. All rights reserved.
doi:10.1016/j.jvolgeores.2005.07.006

about what is happening inside a volcano leading up to and during eruptions. On land, uplift or subsidence of the ground can be measured by leveling surveys, the Global Positioning System (GPS), or interferometric synthetic aperture radar (InSAR) (Dvorak and Dzurisin, 1997; Segall and Davis, 1997; Zebker et al., 2000; Dzurisin, 2003). However, since none of these methods can be used underwater, new techniques have been developed to monitor vertical deformation on submarine volcanoes. To date, the most promising technique has been the use of bottom pressure recorders (BPRs), instruments that continuously record ambient pressure, as a proxy for seafloor depth (Fox, 1999; Fujimoto et al., 2003; Watanabe et al., 2004). These measurements use sea level as a datum so that any uplift or subsidence of the seafloor causes a corresponding decrease or increase in measured pressure, respectively. Other techniques that have been developed for making geodetic measurements on the seafloor include: direct acoustic ranging between pairs of instruments (Chadwell et al., 1999; Chadwick et al., 1999; Nagaya et al., 1999; Chadwick and Stapp, 2002), combined GPS/acoustic positioning of instruments on the bottom from surface ships (Chadwell et al., 1995; Fujimoto et al., 1998; Spiess et al., 1998; Hildebrand et al., 2000; Fujita et al., 2003; Osada et al., 2003), and seafloor gravity measurements (Eiken et al., 2000; Sasagawa et al., 2003).

The longest monitoring record using BPRs at a submarine volcano is at Axial Seamount (Fig. 1), located on the Juan de Fuca Ridge about 270 miles west of the Oregon coast. Axial Seamount is the site of the NeMO seafloor observatory operated by the National Oceanic and Atmospheric Administration (NOAA) (Embley and Baker, 1999, see also http://www.pmel.noaa.gov/vents/nemo/). Between 1987 and 1998, BPRs were deployed each year within the summit caldera of Axial Seamount and on several occasions small deflation events (10 cm or less in magnitude) were measured (Fox, 1990, 1993), some of which were coincident with earthquake swarms (Dziak and Fox, 1999b). Then in January 1998, Axial Seamount experienced a major dike intrusion and eruption (Dziak and Fox, 1999a; Embley et al., 1999). At that time, two BPR instruments were in place at Axial when a large volume of magma moved from the summit reservoir into the south rift zone, resulting in dramatic deflation of the summit. During

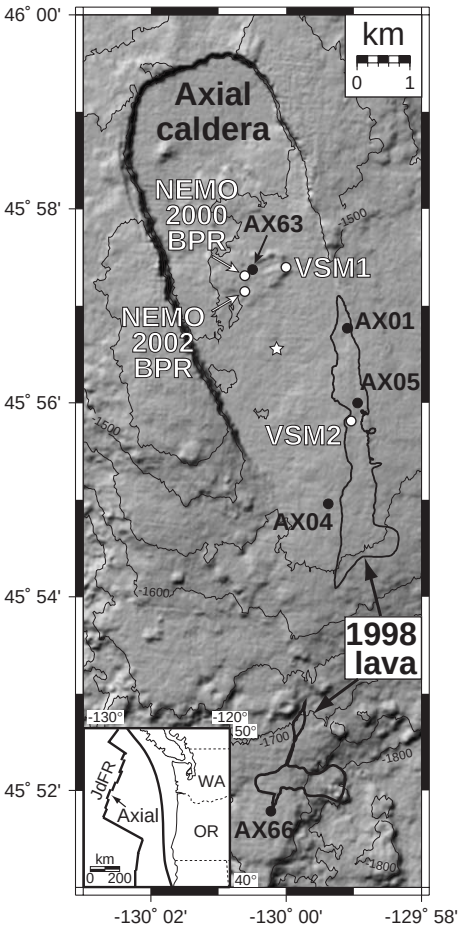

Fig. 1. Map of Axial caldera showing locations of BPRs (white dots) and seafloor benchmarks for MPR measurements (black dots) in relation to the 1998 lava flows (black outlines). Additional information is provided in Tables 1 and 2. Inset shows location of Axial Seamount in relation to the Juan de Fuca Ridge. Best fit Mogi inflation source for MPR measurements between 2000 and 2004 is located at white star.

the first 5 days of the eruption, the BPR located near the center of the volcano's caldera (VSM1, Fig. 1) measured a subsidence of 3.2 m (Fox, 1999), and the other BPR located near the 1998 eruption site (VSM2, Fig. 1) measured a 1.4 m subsidence (Fox et al., 2001). Mechanical modeling of these and other data show that the observed surface deformation can be explained by the removal of 207×10^6 m^3 of magma from a reservoir located 3.8 km beneath the center of the caldera (Chadwick et al., 1999; Fox et al., 2001). In addition, the VSM2 BPR was actually caught in the 1998 lava and directly measured ~3 m of rapid flow

inflation and subsequent lava drainout (Fox et al., 2001; Chadwick, 2003). Since the 1998 eruption, there has been very little seismic activity recorded at Axial (Dziak and Fox, 1999a; Sohn et al., 2004, R. Dziak, personal communication, 2004).

The pressure data collected at Axial Seamount show that BPRs are very good at measuring sudden deflation events, because the pressure sensors have high vertical resolution (~1 mm) over short periods of time (seconds to days). However, measuring gradual volcano inflation with BPRs over longer periods of time (months to years) is potentially problematic, because they can have an inherent instrumental drift which can be difficult to distinguish from any real signal occurring at about the same rate. In an attempt to overcome this problem an independent method has been developed using a mobile pressure recorder (MPR) connected to a remotely operated vehicle (ROV) to make campaign-style pressure measurements on an array of seafloor benchmarks. The relative depths of the benchmarks are determined over a short period of time (hours–days) and these differential measurements have been repeated annually to see if stations inside the caldera are moving up relative to a station outside the caldera that is assumed to be stable. In this paper, BPR data collected at Axial since its 1998 eruption and the results from the MPR measurements are presented, both of which suggest that Axial Seamount has been re-inflating since its 1998 eruption.

2. Field methods and evaluation of results

In this section, the methods used to measure vertical ground deformation at Axial Seamount are described and the results are evaluated, first for the continuous BPR instruments and then for the annual "campaign-style" MPR measurements.

2.1. BPR methods

The continuously recording BPRs used at Axial Seamount (Fig. 2a) were built by NOAA's Pacific

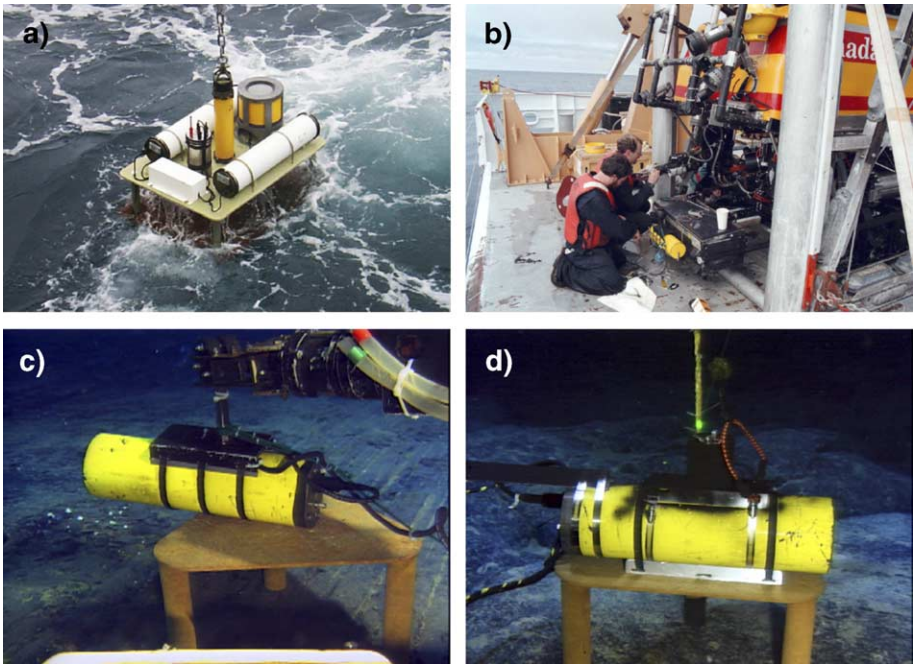

Fig. 2. Photographs of instruments used at Axial Seamount to measure vertical deformation. (a) BPR being deployed, (b) MPR mounted on the front of the remotely operated vehicle ROPOS, (c) MPR held by the ROPOS manipulator arm during a pressure measurement on benchmark AX05 in 2003, and (d) MPR released by the ROPOS arm on benchmark AX63 during a pressure measurement in 2004. The minor change in method in (c) vs. (d) made the orientation of the MPR on the benchmarks more repeatable and significantly reduced the measurement error.

Marine Environmental Laboratory and were originally developed to detect tsunami waves in the deep ocean (Eble et al., 1989; Eble and Gonzalez, 1991; Gonzalez et al., 1991), but have also been used to model tides and subtidal pressure fluctuations (Mofjeld et al., 1995, 1996). The instruments are battery powered, autonomous, and record every 15 s. They are deployed as small moorings from a ship, are anchored to the bottom, and then are recovered 1 to 2 years later using an acoustic release. The BPRs use Paroscientific Digiquartz pressure transducers (model 410K), which apply external pressure to a quartz crystal resonator in a mechanical apparatus called a Bourdon tube (Eble and Gonzalez, 1991; Boss and Gonzalez, 1994). Bourdon tube sensors have a lower drift rate than earlier bellows-type sensors (Wearn and Larson, 1982; Watts and Kontoyiannis, 1990). When the data are processed the measured frequency is converted to psi using temperature and clock corrections, and the pressure in psi can then be converted to depth in meters. The sensors measure absolute pressure and so the converted depths include the contribution from atmospheric pressure. The ocean tidal signal is removed by low-pass filtering in either the time or frequency domains (Eble and Gonzalez, 1991).

In the signal that remains, there can be a long-term instrumental drift at a rate of up to 150 ppm, equal to 23 cm/year at 1530 m, the depth of Axial Seamount's caldera floor (Watts and Kontoyiannis, 1990; Fujimoto et al., 2003, C. Meinig, personal communication, 2003). Therefore, large and/or sudden vertical deformation of the seafloor is obvious in BPR records, but if the deformation is slow, gradual, and within the range of potential instrument drift, it is more difficult to identify unambiguously. The exact rate of drift is specific to each sensor. Drift is typically most acute during the first days or weeks of a deployment while the sensor equilibrates, and then it stabilizes to a lower rate (Eble et al., 1989; Fox, 1990). In addition, the drift rate is less if the measured pressure is a small percentage of their full dynamic range (Wearn and Larson, 1982; Watts and Kontoyiannis, 1990, C. Meinig, personal communication, 2003). For example, Fujimoto et al. (2003) estimated the drift rate of the Paroscientific pressure sensors they used on the southern East Pacific Rise to be 6–12 cm/year based on previous field tests. The long deployment times (1–2 years) and ambient pressures of only a quarter of the full dynamic range of the sensors (mostly 10000 psi or ~6800 m, Table 1) should help to minimize the rate of drift in the BPRs used at Axial.

2.2. BPR results

Since the 1998 eruption, a series of BPRs have recorded pressure data at Axial Seamount (Fig. 1, Table 1). Two instruments were in place during the 1998 eruption, VSM1 located near the center of the caldera which recorded for 10 months, and VSM2 located about 3 km southeast of the center which recorded for 20 months. Unfortunately, between May 1999 and July 2000, no BPR data were recorded at Axial because the instruments that had been previously used there were phased out and it took time for them to be replaced. BPR monitoring resumed in July 2000 with new instruments capable of recording for 2 years (NeMO2000 and NeMO2002, Fig. 1). The NeMO2002 BPR was equipped with an acoustic modem and sent data back to shore hourly via a buoy-based communication system called NeMO Net (Stalin et al., 2001; Chadwick et al., 2002, see also http://www.pmel.noaa.gov/vents/nemo/realtime/).

Table 1
BPRs deployed at Axial Seamount since the 1998 eruption

Name (and alternates)	Dates of deployment	Location of deployment[a]	Depth of deployment (m)	Sensor serial numbers/dynamic range (psi)
VSM1 (WC81)	Oct 3, 1997–Aug 7, 1998	Caldera center 45°57.4′N 130°00.0′W	1535	40,992/10,000
VSM2 (WC82)	Oct 3, 1997–May 5, 1999[b]	1998 lava flow 45°55.81′N 129°59.04′W	1524	57,429/10,000
NeMO2000	Jul 6, 2000–Jul 19, 2002	Caldera center 45°57.31′N 130°00.60′W	1530	73,461/10,000
NeMO2002	Jul 22, 2002–Jul 18, 2004	Caldera center 45°57.15′N 130°00.61′W	1535	87,619/3000

[a] See Fig. 1 for map of deployment locations.
[b] VSM2 ran out of memory on May 5, 1999, and was recovered on July 6, 1999.

The VSM1 BPR that was in place at the center of the caldera during the 1998 eruption recorded a dramatic subsidence of 3.2 m between 25 and 30 January (Fox, 1999). However, immediately after the eruption-related deflation, a signal consistent with long-term inflation began and continued until the instrument was recovered on 7 Aug 1998 (Fig. 3a). Between 30 January and 7 August 1998 the BPR measured 50 cm of apparent uplift in 180 days (an average rate of 101 cm/year), a signal clearly larger than the potential rate of instrumental drift. Another indication that this signal is real is that the rate of inflation was initially high and decreased with time; it was 20 cm/month (240 cm/year) in the first month after the eruption, 10 cm/month (120 cm/year) in the second month, and then 5 cm/month (60 cm/year) over the next 4 months until it was recovered (Fig. 3a). This pattern of quasi-exponentially decreasing rates is consistent with the character of volcanic inflation observed immediately after eruptions on land, apparently reflecting declining hydraulic pressure and recharge rate into the summit magma reservoir with time (Dvorak and Okamura, 1987; Dvorak and Dzurisin, 1993; Lu et al., 2003; Sturkell et al., 2003).

The VSM2 BPR that became stuck in the 1998 lava flow in the SE part of the caldera (Fig. 1) recorded a rapid subsidence of 1.4 m associated with the eruption (Fox et al., 2001). The VSM2 BPR experienced only 40% of the subsidence recorded by the VSM1 BPR because the VSM2 instrument was located 3.5 km from the center of the caldera and the presumed locus of maximum vertical displacement (Fig. 4a). Likewise, immediately after the eruption when deflation abruptly changed to inflation, VSM2 recorded a more modest rate of 22 cm/year of apparent uplift. This rate is near the maximum range of potential instrumental drift. However, the pattern of an initially high rate of inflation that declines with time that was seen in the VSM1 data is also evident in the VSM2 record (Fig. 3b), suggesting that it too is probably real. In addition, the apparent inflation recorded by VSM2 is more or less consistent with the same deformation model that fit the displacements during the eruption (Fig. 4b). The VSM2 BPR

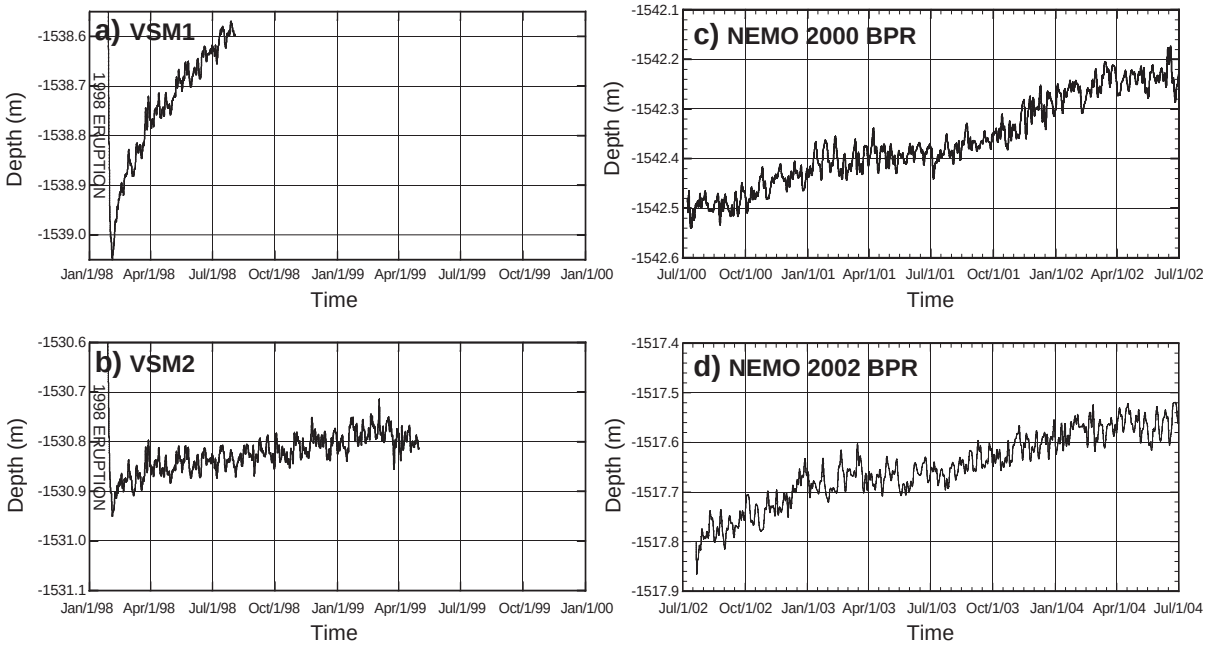

Fig. 3. Plots of BPR data at Axial Seamount showing evidence of inflation (decreasing seafloor depth with time). All plots are shown at the same scale (0.5 m along the *y*-axis and 2 years along the *x*-axis). Data from (a) VSM1 and (b) VSM2 are shown immediately after the abrupt subsidence during the January 1998 eruption. Data from (c) NeMO2000 and (d) NeMO2002 BPRs begin after a 14-month gap in monitoring. Note BPRs in (a), (c), and (d) were all located at or near the center of the caldera, whereas the BPR in (b) was located in the SE part of the caldera (see Fig. 1).

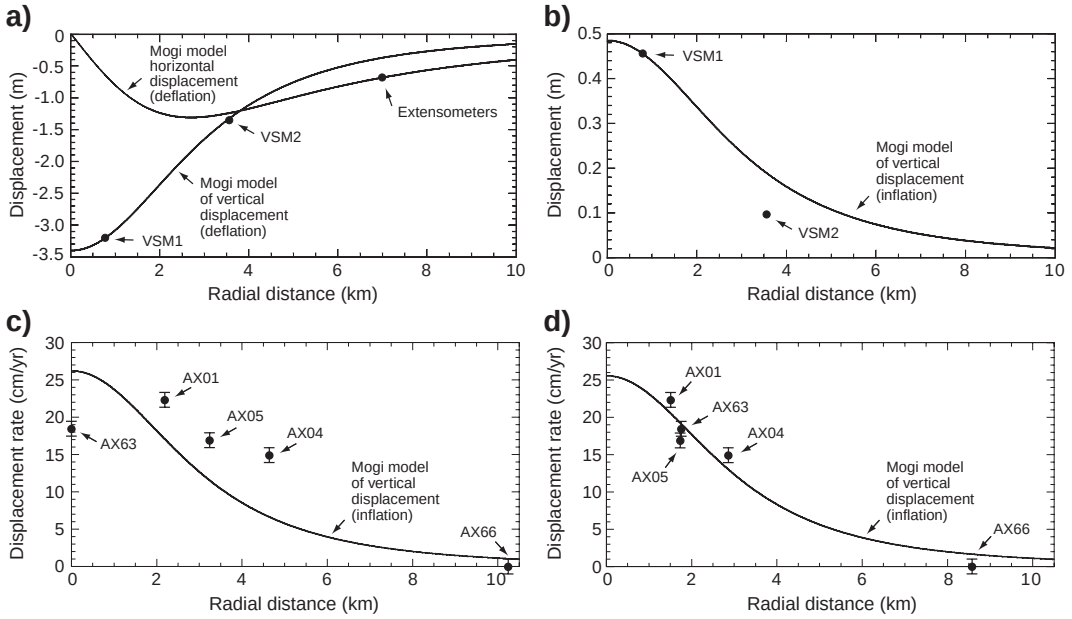

Fig. 4. Plots of BPR and MPR data compared to the Mogi deformation model. (a) The large deflation observed during the 1998 eruption (25–30 January) closely matched displacements predicted by the model located beneath the center of the caldera. (b) Uplift observed by the VSM1 and VSM2 BPRs in the first 6 months after the 1998 eruption (February–August). (c) Comparison of MPR data with a Mogi source located at the center of the caldera (AX63 in Fig. 1). Average rates of inflation from 2000–2004 are shown relative to benchmark AX66, which is assumed to be stable. (d) 2000–2004 MPR data plotted with a Mogi source that minimizes the misfit between the data and the model. In this case, the source location is between AX63 and AX01 (white star in Fig. 1). All Mogi sources are at a depth of 3.8 km. No extensometer data are available after the 1998 eruption to compare with the models in (b–d). Locations of instruments and benchmarks are shown in Fig. 1.

continued to record until May 1999 (9 months longer than VSM1).

Unfortunately, after VSM2 stopped recording, there was a gap in BPR monitoring at Axial Seamount until July 2000 when a new instrument was deployed at the center of the caldera. The NeMO2000 BPR was in place for 2 years until July 2002 and recorded 15 cm/year of apparent uplift during that time period (Fig. 3c). The NeMO2002 BPR was deployed from July 2002 to July 2004 and recorded the same 15 cm/year rate of apparent uplift (Fig. 3d). These rates since 2000 are low enough in magnitude that there is ambiguity as to whether part or all of the signal could be instrumental drift instead of real seafloor uplift. However, the fact that the BPR records from 2000–2004 follow real inflation between 1998 and 1999 and both BPRs show a similar rate of uplift despite having different pressure sensors (which would not be expected to have the exact same rate of drift) suggests that these signals may also represent real vertical deformation.

In summary, a clear inflation signal was recorded by BPRs in the first 6 months after the 1998 eruption, apparently with a locus of maximum uplift near the center of the caldera. The observed rate of uplift immediately after the eruption began at about 10 times the expected rate of instrument drift, and decreased with time in a manner similar to documented volcanic inflation observed on land. After a gap in monitoring, inflationary signals have continued to be recorded at the center of Axial caldera at a lower and relatively constant rate that is within the range of possible instrumental drift, and so is more ambiguous. On the other hand, it is clear that there have been no abrupt deflation events while BPRs were deployed since the 1998 eruption, consistent with the lack of detected seismicity.

2.3. MPR methods

Since 2000, we have been developing an independent method to measure gradual volcanic inflation on

Table 2
MPR benchmark names and locations at Axial Seamount

Name	Location	Position	Depth (m)	Radial distance (m) from caldera center
AX63	Caldera center	45°57.309′N 130°00.603′W	1530	0
AX01	Magnesia	45°56.773′N 129°59.094′W	1524	2199
AX05	Marker 33	45°55.995′N 129°58.947′W	1523	3245
AX04	Bag City	45°54.971′N 129°59.367′W	1534	4638
AX66	Pillow mound	45°51.789′N 130°00.223′W	1723	10,243

the seafloor that is analogous to optical leveling or repeated microgravity surveys on land. The method involves making campaign-style measurements at an array of seafloor benchmarks with a mobile pressure recorder (MPR) carried by an ROV to determine the relative depths of the benchmarks. At Axial, the depths of four benchmarks inside the caldera were determined each year to see if they were moving up or down relative to a benchmark located ~10 km from the center of the caldera, and assumed to be stable (AX66 in Fig. 1).

The MPR instrument consists of two Paroscientific pressure gauges, along with a microcontroller and support electronics. Having multiple pressure sensors allows their output to be compared and averaged to statistically reduce measurement error. The instrument is small enough to be carried and manipulated by an ROV (Fig. 2b), and a direct electrical connection allows data to be evaluated on the ship in real-time. These campaign-style pressure measurements were begun at Axial in 2000 and have been repeated each year through 2004.

The seafloor benchmarks used at Axial consist of triangular flat plates made out of galvanized steel, 46 cm on a side, with three 25-cm-high legs, and weighing 20 pounds in water (Fig. 2c and d). These benchmarks were positioned in flat stable areas on the seafloor using an ROV. Although they are not physically attached to the bottom, they provide adequate vertical stability for the MPR measurements. Lateral movement of the benchmarks is unlikely due to their weight, the benign environment of the deep ocean, and the care taken to not disturb them during measurements. The benchmarks are located at a range of radial distances from the caldera center (Fig. 1 and Table 2) in order to help compare any observed displacements with deformation models.

Each pressure measurement involves simply placing the MPR on the benchmark with the ROV's manipulator arm (Fig. 2c and d) and recording for 20–30 min (enough time to let the pressure sensors stabilize). Making measurements at all 5 benchmarks over a short period of time (hours–days) eliminates the ambiguity of long-term sensor drift. However, short-term drift must still be accounted for and can be quantified by making repeated measurements at benchmarks in a closed-loop survey. The number of repeat measurements has not been the same each year and generally increased with time as the method was refined to reduce measurement errors (Table 3).

This technique was modeled after another study that used repeated pressure and gravity measurements on the seafloor to document seafloor subsidence over an oil and gas reservoir in the North Sea (Eiken et al., 2000; Sasagawa et al., 2003). In that study, a repeat-

Table 3
Characteristics of MPR surveys in different years and residual errors

Year	Sensor serial numbers (gauge1/gauge2)	Number of transects	Number of repeat measurements at each benchmark					Computed error (cm) (standard deviation of residuals)
			AX63	AX01	AX05	AX04	AX66	
2000	43,886/53,344[a]	1	1[b]	1	1	1	2[b]	15.0
2001	43,526/43,535	2	2[b]	1	1	2	1	5.6
2002	62,201/43,535	3	2	3	3	2	2[b]	5.1
2003	62,201/43,535	3	2	3	3	3	2[b]	3.2
2004	62,201/43,535	3	2	3	3	3	2	0.9

[a] Pressure gauge SN 53344 did not give reliable results in the 2000 survey.
[b] During the first measurement, pressure gauges probably were not thermally equilibrated.

ability of about 1 cm was achieved in determining the relative heights between 77 seafloor benchmarks at ~320 m depth. This value was obtained by computing the standard deviations of repeated stations and then averaging them (Eiken et al., 2000; Sasagawa et al., 2003).

2.4. MPR data processing

After the MPR data are converted to depth in meters, corrections are made by subtracting the combined effect of ocean surface tide and air pressure variation measured by a local BPR (although the 2004 data were corrected with a tide model because BPR data are not yet available). A depth from each of the two pressure gauges is picked from each benchmark occupation. Next, the average depth at each benchmark (from all occupations) is calculated and subtracted from each depth measurement at that benchmark and a common drift is fit simultaneously for all the sites with repeated measurements (Fig. 5). The calculated short-term drift rates each year ranged from 1 to 8 cm/day. As expected, these rates are much higher than for the BPRs because the sensors in the MPR are subjected to highly variable conditions during ROV motions and manipulator handling. The final depth for each benchmark occupation is the average of the drift-corrected depths from both gauges.

After correcting for drift, the average depth values at all repeated benchmarks (in that year's survey) are subtracted from the individual measurements. The deviation from zero of these residual values indicates the level of noise in that year's survey. The standard deviation of the residual depths is adopted as the error for a given survey, since this is the best estimate of the repeatability of the measurements (Table 3).

2.5. MPR error analysis

The repeatability of the MPR measurements has improved as sources of error have been progressively identified and eliminated each year. The standard deviations of the residuals were 15 cm in 2000, 5.6 cm in 2001, 5.1 cm in 2002, 3.2 cm in 2003, and 0.9 cm in 2004. The errors in 2000 were much higher because only one of the two pressure gauges worked reliably that year and repeat measurements were made at only 1 of the 5 benchmarks (whereas they have been made at all benchmarks since 2002; Table 3). The error budget for the MPR measurements is outlined in Table 4. The known sources of error include the inherent depth resolution of the pressure gauges, calibration uncertainty, and background noise. In 2000–2003, there is also uncertainty in the recorded start times for the benchmark occupations of up to 2 min, which could cause a phase offset in the tidal

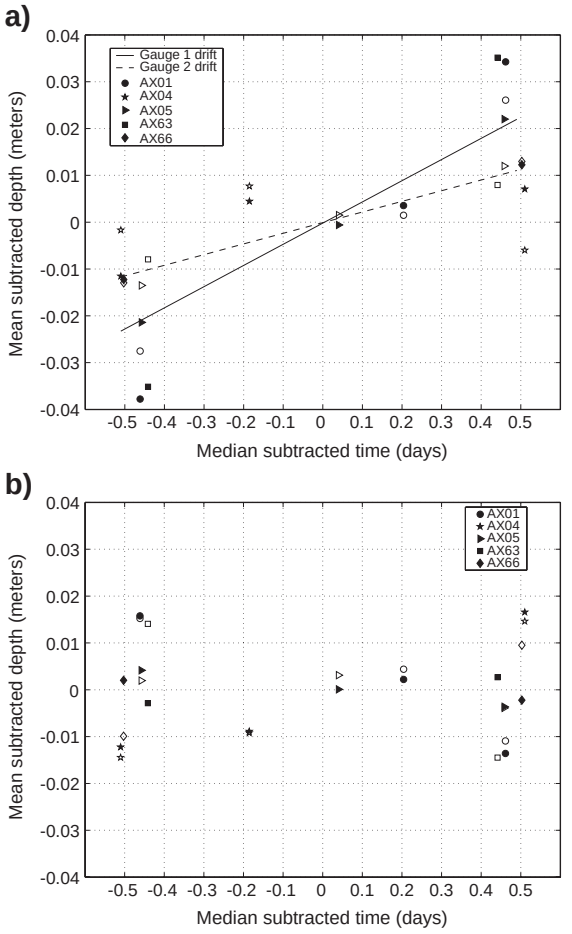

Fig. 5. (a) Plot of the depth values from repeated stations used to calculate a drift rate during the 2004 MPR survey. For each benchmark, the mean is subtracted from the depths at that station on the *y*-axis, and the median is subtracted from the measurement times at that station on the *x*-axis. This puts all the measurements at different stations in the same reference frame so they can be readily compared. Filled and unfilled symbols are from the two different pressure gauges inside the MPR instrument. The calculated drift rates are 4.5 cm/day for gauge 1 and 2.3 cm/day for gauge 2. (b) Same plot after the short-term drift has been removed. This figure shows the level of repeatability at each benchmark during the 2004 survey.

Table 4
Error budget for the 2003 MPR measurements

Error source	Depth uncertainty 2000 (cm)	Depth uncertainty 2001–2002 (cm)	Depth uncertainty 2003 (cm)	Depth uncertainty 2004 (cm)
Inherent precision of the gauges	0.1	0.1	0.1	0.1
Background noise	0.6	0.6	0.6	0.4
Calibration uncertainty	0.5	0.5	0.5	0.5
Tide correction uncertainty	2.0	2.0	2.0	1.2
Drift correction	5.0	0.7	0.7	0.3
Depth conversion uncertainty	0.5	0.5	0.5	0.5
Rotational uncertainty	5.0	5.0	1.5[a]	0.1
RMS sum of errors	7.4	5.5	2.8	1.5
Observed repeatability	15.0	5.6, 5.1	3.2	0.9

[a] Errors reduced by rotation corrections applied based on laboratory test results.

corrections. Since the maximum tidal rate of change is about 1 cm/min, this could lead to an error of at most 2 cm. Benchmark instability is not likely to be a significant source of error, because at each site the benchmarks are sitting on solid and relatively flat seafloor lavas (Fig. 2c and d).

Between the 2003 and 2004 field seasons, laboratory tests were conducted with the MPR instrument under pressure. These tests identified two other key sources of error that had been previously overlooked. First, the output of the Paroscientific pressure gauges was found to depend strongly on their orientation relative to the Earth's gravitational field (Fig. 6), and therefore small rotations of the pressure sensor from one measurement to another were a major source of error in our 2000–2003 measurements (Table 4). Before 2004, when the MPR was placed on a seafloor benchmark, it was oriented by eye so that the ROV handle appeared to be vertical, the long-axis of the MPR was flush with the flat surface of each benchmark, and the endcap was near the center of the benchmark (Fig. 2c). The MPR handle is estimated to have been placed within 10° of vertical during each benchmark occupation, which translates to an error of ±5 cm (Fig. 6 and Table 4).

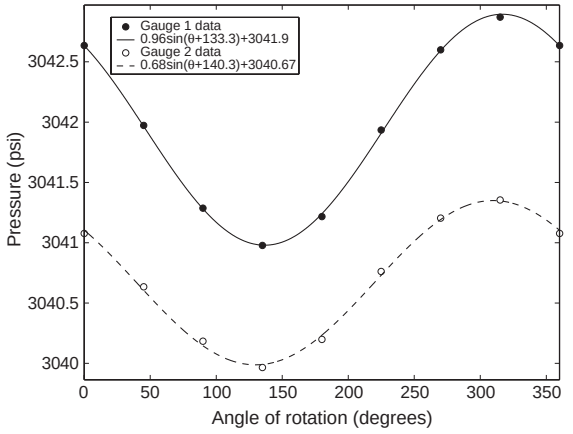

Fig. 6. The results of a laboratory test of the MPR instrument under pressure showing the variation of the output from the two Paroscientific pressure gauges (converted to psi) as a function of rotation of the instrument about its long axis. The pressure was held constant (3041.64 psi) with a dead-weight calibrator while the sensor was rotated.

As a solution to this problem, the following steps were taken in 2004 to minimize tilt changes between measurements and to make the exact position of the instrument more repeatable at each benchmark: 1) a flat plate was attached to the bottom of the MPR so that it was self-righting and the ROV could release it during measurements, 2) the MPR was positioned in the same orientation during each occupation at a given site, parallel with one of the sides of the triangular benchmarks (Fig. 2d), 3) tilt sensors were added to the MPR instrument and both tilt and pressure readings were displayed on the ship in real-time during measurements, and 4) the pressure sensors were oriented inside the MPR in such a way that their response to rotation was minimized (near the peaks of the sinusoid in Fig. 6).

The second source of error discovered during the lab test was that the pressure sensors do not become thermally equilibrated until about 2 h at ambient seafloor temperature (~3 °C). This means that the first pressure measurement during previous years' dives was usually made before the gauges had

thermally equilibrated, contributing an additional error that is difficult to quantify. The solution to this problem (implemented in 2004) is simply to wait for 2 h before making the first pressure measurement during a dive or to thermally equilibrate the pressure sensor in an ice bath on deck before deployment.

Compounding this problem, our first measurements in 2000–2003 were often made at our reference station outside the caldera (Table 3), meaning this error contaminated all the other measurements during that year (since the pressure at stations inside the caldera is measured relative to the reference station). Additionally, the reference benchmark was never measured more than twice per survey. Since both measurements were also affected by an unknown gauge rotation (as discussed above), the second measurement provided little constraint on the uncertainty of that benchmark. Together, these two factors made the possible error in the reference benchmark larger than the survey repeatability would suggest. This is the most likely source of the systematic year-to-year depth variations that are correlated between sites during 2000–2003. For example, in Fig. 7 all the points in 2002 are significantly above the average rate lines, and the points in 2001 and 2003 are all below the lines. This problem illustrates the importance of measurements at the reference benchmark.

The 2004 results show that the changes implemented to reduce the errors identified during the laboratory tests improved our repeatability dramatically to less that 1 cm (Table 4, Fig. 7), and indicate that the MPR method has finally matured. The laboratory tests also showed that the two pressure gauges used in the MPR instrument have slightly different response amplitudes to rotation (Fig. 6). This allowed us to back-calculate rotation corrections for the 2003 MPR measurements (Fig. 7 and Table 4), since the orientation of the gauges inside the instrument in 2003 was the same as during the lab test.

2.6. MPR results

The year-to-year results from the MPR measurements show apparent inflation at all four benchmarks inside the caldera relative to the benchmark outside the caldera, which is assumed to be stable. The MPR measurements, weighted by their uncer-

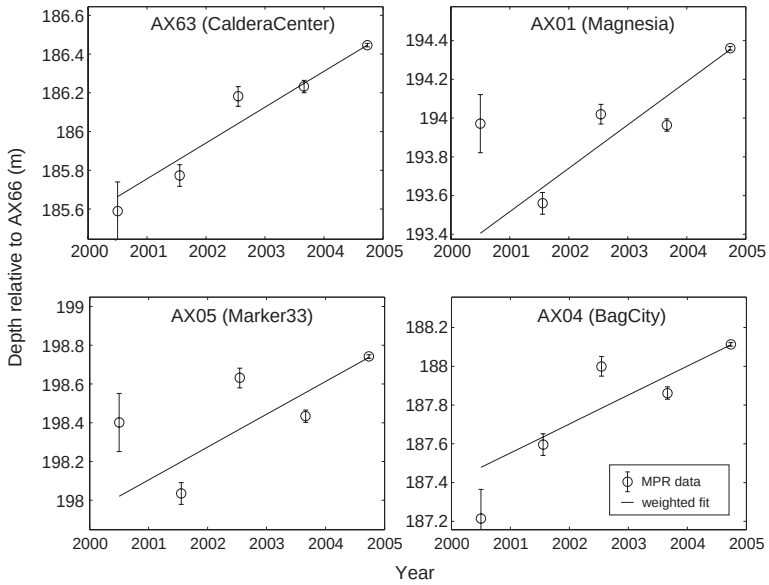

Fig. 7. MPR results between 2000 and 2004 showing the depth of the four benchmarks in Axial caldera vs. time relative to benchmark AX66 located outside the caldera, which is assumed fixed at a relative depth of zero (its actual depth is −1723 m). The average rates (lines) are least squares fits inversely weighted by the errors (see Tables 4 and 5). Note the error bars are smaller than the symbol size in 2004. Locations of the benchmarks are shown in Fig. 1.

tainties, are fit to a linear trend at each site in Fig. 7. The average rate of uplift of the center of the caldera (AX63) is 19 ± 1.3 cm/year. This formal uncertainty in the slope, based on the individual error bars and the observation time, is consistent with the standard deviation of the residuals to the fit (9.0 cm) and the 4 year time span of the MPR experiment (Table 5). The slope compares favorably with the apparent uplift rate of ~15 cm/year as measured by the BPR instruments deployed at the caldera center during that time. This agreement between two independent methodologies gives us more confidence in the reliability of each.

The average rates of uplift at the other three benchmarks (Fig. 7 and Table 5) are either somewhat higher (AX01) or lower (AX05 and AX04). The dramatic subsidence observed in Axial caldera by the two BPRs during the 1998 eruption fit a simple deformation model (Fig. 4a) with a Mogi point-source at 3.8 km depth beneath the center of the caldera (Mogi, 1958; Chadwick et al., 1999; Fox et al., 2001). The fit of the pattern of uplift rates from the MPR measurements since 2000 to the Mogi model (with the same source depth and location) is not as good, however (Fig. 4c). The fact that the average rate of inflation is greater at AX01 than at AX63 suggests the possibility that the location of maximum uplift during 2000–2004 was not at the center of the caldera, but instead was closer to AX01. The Mogi solution which minimizes the misfit between the data and the model has a source located 1.8 km SSE of the caldera center (Figs. 1 and 4d). The previously determined source depth of 3.8 km is still consistent with the data, although it is not tightly constrained.

Table 5
MPR results (average rates of vertical displacement)

Benchmark	2000–2004 (weighted as a function of error)	
	Average rate (cm/year)	Standard deviation of residuals (cm)
AX63	18.5 ± 1.3	9.0
AX01	22.4 ± 1.3	28.4
AX05	16.9 ± 1.3	24.0
AX04	14.9 ± 1.3	17.9

These rates are the best fit lines presented in Fig. 7. Note all displacements are relative to benchmark AX66, which is assumed to be fixed (zero vertical displacement). The third column shows the standard deviation of the residuals after subtracting the best fitting line and is a measure of how well a linear model fits the data.

Note that the standard deviations of the residuals in Table 5 (other than for AX63) are not consistent with the formal slope uncertainty (they should be about 4 times greater for the 4 year time period). The two sites most inconsistent with a linear inflation rate (AX01 and AX05) are also the two within the area of 1998 lava (Fig. 1). This may suggest that deformation on the 1998 lava flow has been more complex. However, if the 2000 data are not included, the standard deviation of the residuals drops to ~13 cm for AX01 and AX05. This plus the uncertainty in the reference benchmark prior to 2004 indicates that the imperfect fit to the linear trend probably reflects unaccounted for noise in the earlier measurements. The data from the caldera center (AX63) seems to have the best signal-to-noise ratio (Fig. 7 and Table 5), but there is no reason to have less confidence in the measurements made at the other benchmarks. In any case, more confidence can be placed in the long-term average trends than in the specific changes from year-to-year.

3. Discussion

The BPR results confirm that continuously recording pressure sensors are excellent tools for measuring vertical displacements of the seafloor. Low or gradual deformation rates that are within the range of possible instrumental drift are difficult to identify unambiguously, but can potentially be verified by others methods. The MPR results show that campaign-style pressure measurements are a viable method to independently measure gradual volcano inflation on the seafloor.

Together, the BPR and MPR monitoring data from Axial Seamount suggest that inflation has been occurring since its 1998 eruption at a rate that was initially high and gradually decreased to a more steady rate. This interpretation is strongest immediately after the eruption when uplift rates (>100 cm/year) were well above potential BPR drift rates (<23 cm/year), but becomes less certain as the rates decrease to lower levels (15–20 cm/year). However, it appears that these lower rates are caused by uplift, rather than instrument drift, for the following reasons: 1) they are consistent with an expected decreasing uplift rate,

2) the same rate of uplift was observed by two independent BPR instruments (which should not necessarily have the same drift characteristics), 3) the drift rate of the BPRs at Axial is probably well below the expected maximum because of their long deployment times and low pressure exposure relative to their dynamic range, and 4) the BPR results generally agree with the rate of uplift observed by the independent MPR measurements.

If one accepts the pressure data as showing real uplift, a long-term view of inflation at Axial Seamount can be assembled. Fig. 8 combines all the BPR and MPR results from the center of Axial caldera in one plot by making a few key assumptions. First, the depth values of the NeMO2000 and NeMO2002 BPR data were shifted so that, 1) the rate of uplift observed in 2000–2004 (15 cm/year) extends back to August 1998 when VSM1 was recovered, 2) the NeMO2002 data start at the same depth at which the NeMO2000 data end, and 3) the MPR data are overlain on the BPR data by aligning the 2001 MPR measurement with the underlying NeMO2000 BPR data (which is reasonable because they were co-located at the time).

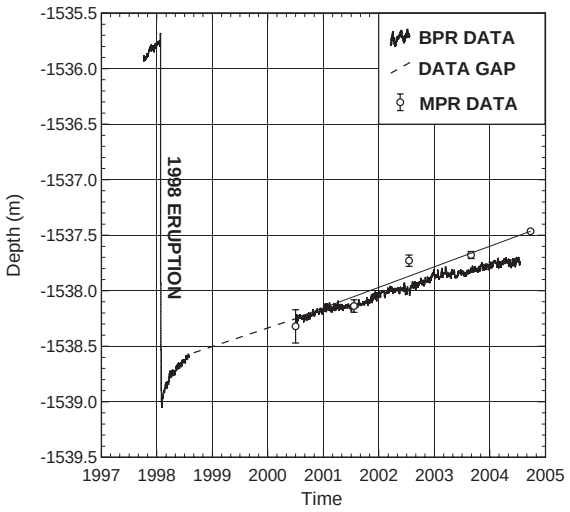

Fig. 8. Interpretive plot of BPR and MPR data showing inflation at the center of the caldera since the 1998 eruption (BPR data include VSM1, NeMO2000, and NeMO2002; MPR data are from benchmark AX63). This plot is speculative because the individual BPRs do not share a common datum or location and the MPR measurements are relative (see text for discussion). Nevertheless, the BPR and MPR results appear to be consistent with each other and suggest that the caldera center has been uplifted by 1.5 ± 0.1 m since the 1998 eruption. The plot was assembled by assuming that the same rate of inflation observed by the NeMO2000 BPR in 2000–2002 had been occurring during the data gap since August 1998 (dashed line). The MPR data were overlain on the BPR data by co-registering the two in 2001 when they were co-located (the AX63 benchmark was within a few meters of the NeMO2000 BPR). The straight solid line is the average uplift rate from the MPR data, as in Fig. 7. The MPR error bar for 2004 is smaller than the symbol size.

The combined results in Fig. 8 indicate that since the 1998 eruption, the center of Axial caldera has been uplifted 1.5 ± 0.1 m in 6.7 years (as of September 2004). In other words, almost 50% of the 3.2 m of subsidence that occurred during the 1998 eruption has been recovered to date. If inflation continues at the current rate of 19 cm/year at the caldera center, it will take another 9 years (16 years total) for the caldera to fully re-inflate to its January 1998 level (or in about 2014). If one assumes that Axial would then be poised to erupt again, such a recurrence interval (~16 years), although admittedly speculative, would not be unreasonable since it is also the time necessary to accumulate ~1 m of extensional strain (the mean thickness of dikes seen in ophiolites (Kidd, 1977) and tectonic windows (Karson, 2002)) at the Juan de Fuca Ridge's spreading rate of 6 cm/year (Riddihough, 1984).

The change in volume of the magma reservoir beneath Axial caldera required to cause 1.5 m of uplift can be estimated as 91×10^6 m^3, assuming the reservoir is spherical (Johnson, 1992; Delaney and McTigue, 1994) and ignoring any compression of stored magma (Johnson et al., 2000). This volume change over 6.7 years suggests an average magma supply rate at Axial Seamount of 14×10^6 m^3/year. For comparison, this rate is 3–6 times lower than the long-term average magma supply rate of $50–90 \times 10^6$ m^3/year estimated for Kilauea Volcano, Hawaii (Dzurisin et al., 1984; Dvorak and Dzurisin, 1993).

Long-term deformation monitoring from basaltic volcanoes on land, like Kilauea, Hawaii, or Krafla, Iceland, show that brief periods of sudden deflation associated with intrusions or eruptions are often separated by longer periods of gradual inflation during which magma is stored in centralized reservoirs (Björnsson et al., 1979; Decker, 1987; Tilling and Dvorak, 1993). During these periods of inflation, the center of uplift can migrate laterally as much as

several kilometers, apparently due to non-ideal geometry and complex refilling within the magma reservoir (Fiske and Kinoshita, 1969; Ewart et al., 1991). Recent tomographic and multichannel seismic data show that a large magma reservoir exists beneath the summit caldera of Axial Seamount (West et al., 2001; Kent et al., 2003). The deflation observed in the caldera during the 1998 eruption (Fox, 1999; Fox et al., 2001) and the apparent re-inflation observed since then suggest the possibility of an eruption cycle at Axial with a deformation signature similar to those documented on land. Such a cycle has also been suggested by seismo-acoustic monitoring of earthquakes at Axial, which began in 1991 (Dziak and Fox, 1999b). During the 7 years leading up to the 1998 eruption, the frequency and size of small earthquake swarms increased, but since the eruption very few earthquakes have been detected. Therefore, it might be expected that as re-inflation continues and the summit magma reservoir re-pressurizes, that earthquake swarms will once again herald Axial's next eruption. The potential value of vertical deformation monitoring for estimating magma supply rates, forecasting eruptions, and quantifying displacements during eruptions is strong motivation to continue these efforts at Axial Seamount and other active submarine volcanoes.

Acknowledgements

This work was funded by NOAA's West Coast and Polar Regions Undersea Research Center and the NOAA Vents Program. Chris Meinig, Alex Nakamura, and Hugh Milburn from NOAA PMEL's Engineering Development Division designed and built the BPRs deployed at Axial. Scott Stalin designed the NeMO Net communication system that relays BPR data to shore in near real-time. Data processing of the BPR data was performed by Marie Eble and Andy Lau. Special thanks to the ROPOS pilots who carefully executed the MPR measurements. The captains and crews of the *NOAA ship Ronald Brown* and the *R/V Thomas Thompson* skillfully facilitated our instrument deployments, recoveries, and ROV operations at Axial Seamount each year. Thanks also to Theo Schaad at Paroscientific, Inc. for useful discussions about the characteristics of their pressure sensors. This paper was improved by the comments of David Chadwell, Michael Poland, and an anonymous reviewer. PMEL contribution #2709.

References

Björnsson, A., Johnsen, G., Sigurdsson, S., Thorbergsson, G., Tryggvason, E., 1979. Rifting of the plate boundary in north Iceland, 1975–1978. J. Geophys. Res. 84, 3029–3038.

Boss, E.F., Gonzalez, F.I., 1994. Signal amplitude uncertainty of a Digiquartz pressure transducer due to static calibration error. J. Atmos. Ocean. Technol. 11, 1381–1387.

Chadwell, C.D., Spiess, F.N., Hildebrand, J.A., Prawirodirdjo, L., Young, L.E., Purcell, G.H., Dragert, H., 1995. The Juan de Fuca Ridge geodesy project: strain and plate motion measurements using GPS and acoustics. Eos Trans. AGU 76, F412.

Chadwell, C.D., Hildebrand, J.A., Spiess, F.N., Morton, J.L., Normark, W.R., Reiss, C.A., 1999. No spreading across the southern Juan de Fuca ridge axial cleft during 1994–1996. Geophys. Res. Lett. 26, 2525–2528.

Chadwick Jr., W.W., 2003. Quantitative constraints on the growth of submarine lava pillars from a monitoring instrument that was caught in a lava flow. J. Geophys. Res. 108, 2534, doi: 10.1029/2003JB002422.

Chadwick Jr., W.W., Stapp, M., 2002. A deep-sea observatory experiment using acoustic extensometers: precise horizontal distance measurements across a mid-ocean ridge. IEEE J. Oceanic Eng. 27, 193–201.

Chadwick Jr., W.W., Embley, R.W., Milburn, H.B., Meinig, C., Stapp, M., 1999. Evidence for deformation associated with the 1998 eruption of Axial Volcano, Juan de Fuca Ridge, from acoustic extensometer measurements. Geophys. Res. Lett. 26, 3441–3444.

Chadwick Jr., W.W., Butterfield, D.A., Embley, R.W., Meinig, C.S.S., Nooner, S., Zumberge, M., Fox, C.G., 2002. Recent results from seafloor instruments at the NeMO Observatory, Axial Seamount, Juan de Fuca Ridge. Eos Trans. AGU 83 (Abstract T22A-1132).

Decker, R.W., 1987. Dynamics of Hawaiian volcanoes. In: Decker, R.W., Wright, T.L., Stauffer, P.H. (Eds.), Volcanism in Hawaii, U. S. Geol. Surv. Prof. Pap., vol. 1350, pp. 997–1018.

Delaney, P.T., McTigue, D.F., 1994. Volume of magma accumulation or withdrawal estimated from surface uplift or subsidence, with application to the 1960 collapse of Kilauea Volcano. Bull. Volcanol. 56, 417–424.

Dvorak, J.J., Dzurisin, D., 1993. Variations in magma supply rate at Kilauea volcano, Hawaii. J. Geophys. Res. 98, 22255–22268.

Dvorak, J.J., Dzurisin, D., 1997. Volcano geodesy: the search for magma reservoirs and the formation of eruptive vents. Rev. Geophys. 35, 343–384.

Dvorak, J.J., Okamura, A.T., 1987. A hydraulic model to explain variations in summit tilt rate at Kilauea and Mauna Loa volcanoes. In: Decker, R.W., Wright, T.L., Stauffer, P.H. (Eds.), Volcanism in Hawaii, U. S. Geol. Surv. Prof. Pap., vol. 1350, pp. 1281–1296.

Dziak, R.P., Fox, C.G., 1999a. The January 1998 earthquake swarm at Axial Volcano, Juan de Fuca Ridge: hydroacoustic evidence of seafloor volcanic activity. Geophys. Res. Lett. 26, 3429–3432.

Dziak, R.P., Fox, C.G., 1999b. Long-term seismicity and ground deformation at Axial Volcano, Juan de Fuca Ridge. Geophys. Res. Lett. 26, 3641–3644.

Dzurisin, D., 2003. A comprehensive approach to monitoring volcano deformation as a window on the eruption cycle. Rev. Geophys. 41, 1001, doi:10.1029/2001RG000107.

Dzurisin, D., Koyanagi, R.Y., English, T.T., 1984. Magma supply and storage at Kilauea Volcano, Hawaii, 1956–1983. J. Volcanol. Geotherm. Res. 21, 177–206.

Eble, M.C., Gonzalez, F.I., 1991. Deep-ocean bottom pressure measurements in the northeast Pacific. J. Atmos. Ocean. Technol. 8, 221–233.

Eble, M.C., Gonzalez, F.I., Mattens, D.M., Milburn, H.B., 1989. Instrumentation, field operations, and data processing for PMEL deep ocean bottom pressure measurements. NOAA Technical Memorandum ERL PMEL-89. 71 pp.

Eiken, O., Zumberge, M.A., Sasagawa, G., 2000. Gravity monitoring of offshore gas reservoirs. Proceedings of the Society for Exploration Geophysics, Calgary, August 2000.

Embley, R.W., Baker, E.T., 1999. Interdisciplinary group explores seafloor eruption with remotely operated vehicle. Eos Trans. AGU 80, 213, 219, 222.

Embley Jr., R.W., Chadwick, W.W., Clague, D., Stakes, D., 1999. The 1998 Eruption of Axial Volcano: multibeam anomalies and seafloor observations. Geophys. Res. Lett. 26, 2428–3425.

Ewart, J.A., Voight, B., Björnsson, A., 1991. Elastic deformation models of Krafla Volcano, Iceland, for the decade 1975 through 1985. Bull. Volcanol. 53, 436–459.

Fiske, R.S., Kinoshita, W.T., 1969. Inflation of Kilauea volcano prior to its 1967–1968 eruption. Science 165, 341–349.

Fox, C.G., 1990. Evidence of active ground deformation on the mid-ocean ridge: Axial Seamount, Juan de Fuca Ridge, April–June, 1988. J. Geophys. Res. 95, 12813–12822.

Fox, C.G., 1993. Five years of ground deformation monitoring on Axial Seamount using a bottom pressure recorder. Geophys. Res. Lett. 20, 1859–1862.

Fox, C.G., 1999. In situ ground deformation measurements from the summit of Axial Volcano during the 1998 volcanic episode. Geophys. Res. Lett. 26, 3437–3440.

Fox, C.G., Chadwick Jr., W.W., Embley, R.W., 2001. Direct observation of a submarine volcanic eruption from a sea-floor instrument caught in a lava flow. Nature 412, 727–729.

Fujimoto, H., Koizumi, K., Osada, Y., Kanazawa, T., 1998. Development of instruments for seafloor geodesy. Earth Planets Space 50, 905–911, doi:10.1029/2002GL016677.

Fujimoto, H., Mochizuki, M., Mitsuzawa, K., Tamaki, T., Sato, T., 2003. Ocean bottom pressure variations in the southeastern Pacific following the 1997–98 El Nino event. Geophys. Res. Lett. 30, 1456, doi:10.1029/2002GL016677.

Fujita, M., Sato, M., Yabuki, T., Mochizuki, M., Asada, A., 2003. Examination on repeatability of GPS/Acoustic seafloor positioning for the reference points deployed around Japan. Eos Trans. AGU 84 (Abstract G21D-0297).

Gonzalez, F.I., Mader, C.L., Eble, M.C., Bernard, E.N., 1991. The 1987–88 Alaskan Bight Tsunamis: deep ocean data and model comparisons. Nat. Hazards 4, 119–139.

Hildebrand, J.A., Chadwell, C.D., Wiggins, S.M., Spiess, F.N., 2000. Offshore geodetic monitoring on the southeast flank of Kilauea Volcano (abstract). Seismol. Res. Lett. 71, 232.

Johnson, D.J., 1992. Dynamics of magma storage in the summit reservoir of Kilauea volcano, Hawaii. J. Geophys. Res. 97, 1807–1820.

Johnson, D.J., Sigmundsson, F., Delaney, P.T., 2000. Comment on "Volume of magma accumulation or withdrawal estimated from surface uplift or subsidence, with application to the 1960 collapse of Kilauea Volcano" by P. T. Delaney and D. F. McTigue. Bull. Volcanol. 61, 491–493.

Karson, J.A., 2002. Geologic structure of the uppermost oceanic crust created at fast- to intermediate-rate spreading centers. Annu. Rev. Earth Planet. Sci. 30, 347–384, doi:10.1146/annurev.earth.30.091201.141132.

Kent, G., et al., 2003. A new view of 3-D magma chamber structure beneath Axial Seamount and coaxial segment: preliminary results from the 2002 multichannel seismic survey of the Juan de Fuca Ridge. Eos Trans. AGU 84 (Abstract B12A-0755).

Kidd, R.G.W., 1977. A model for the process of formation of the upper oceanic crust. Geophys. J. R. Astron. Soc. 50, 149–183.

Lu, Z., Masterlark, T., Dzurisin, D., Rykhus, R., Wicks Jr., C., 2003. Magma supply dynamics at Westdahl volcano, Alaska, modeled from satellite radar interferometry. J. Geophys. Res. 108, 2354, doi:10.1029/2002JB002311.

Mofjeld, H.O., Gonzalez, F.I., Eble, M.C., Newmand, J.C., 1995. Ocean tides in the continental margin off the Pacific Northwest Shelf. J. Geophys. Res. 100, 10789–10800.

Mofjeld, H.O., Gonzalez, F.I., Eble, M.C., 1996. Subtidal bottom pressure observed at Axial Seamount in the northeastern continental margin of the Pacific Ocean. J. Geophys. Res. 101, 16381–16390.

Mogi, K., 1958. Relations between the eruptions of various volcanoes and the deformation of the ground surfaces around them. Bull. Earthq. Res. Inst. Univ. Tokyo 36, 99–134.

Nagaya, Y., Urabe, T., Yabuki, T., 1999. Crustal deformation observation at the crest of the EPR 18.5S with the seafloor acoustic ranging method. Eos Trans. AGU 80, F1076.

Osada, Y., Fujimoto, H., Miura, S., Sweeney, A., Kanazawa, T., Nakao, S., Sakai, S., Hildebrand, J.A., Chadwell, C.D., 2003. Estimation and correction for the effect of sound velocity variation on GPS/Acoustic seafloor positioning: an experiment off Hawaii Island. Earth Planets Space 55, E17–E20.

Riddihough, R., 1984. Recent movements of the Juan de Fuca plate system. J. Geophys. Res. 89, 6980–6994.

Sasagawa, G., Crawford, W., Eiken, O., Nooner, S., Stenvold, T., Zumberge, M., 2003. A new sea-floor gravimeter. Geophysics 68, 544–553.

Segall, P., Davis, J.L., 1997. GPS applications for geodynamics and earthquake studies. Annu. Rev. Earth Planet. Sci. 25, 301–336.

Sohn, R.A., Barclay, A.H., Webb, S.C., 2004. Microearthquake patterns following the 1998 eruption of Axial Volcano, Juan de Fuca Ridge: mechanical relaxation and thermal strain. J. Geophys. Res. 109, B01101, doi:10.1029/2003JB002499.

Spiess, F.N., Chadwell, C.D., Hildebrand, J.A., Young, L.E., Purcell Jr., G.H., Dragert, H., 1998. Precise GPS/Acoustic positioning of seafloor reference points for tectonic studies. Phys. Earth Planet. Inter. 108, 102–112.

Stalin, S.E., Milburn, H.B., Meinig, C., 2001. NeMO Net: a near real-time deep ocean observatory. Proceedings of the MTS/IEEE Conference and Exhibition, 11–14 September 2000, Providence, RI, pp. 583–587.

Sturkell, E., Einarsson, P., Sigmundsson, F., Hreinsdottir, S., Geirsson, H., 2003. Deformation of Grimsvotn volcano, Iceland: 1998 eruption and subsequent inflation. Geophys. Res. Lett. 30, 1182, doi:10.1029/2002GL016460.

Tilling, R.I., Dvorak, J.J., 1993. Anatomy of a basaltic volcano. Nature 363, 125–133.

Watanabe, T., Matsumoto, H., Sugioka, H., Mikada, H., Suyehiro, K., 2004. Offshore monitoring system records recent earthquake off Japan's Northernmost island. Eos Trans. AGU 85, 14.

Watts, D.R., Kontoyiannis, H., 1990. Deep-ocean bottom pressure measurements. J. Atmos. Ocean. Technol. 7, 296–306.

Wearn, R.B., Larson, N.G., 1982. Measurements of the sensitivities and drift of Digiquartz pressure sensors. Deep-Sea Res. 29, 111–134.

West, M.E., Menke, W., Tolstoy, M., Webb, S., Sohn, R., 2001. Magma storage beneath Axial Volcano on the Juan de Fuca mid-ocean ridge. Nature 413, 833–836.

Zebker, H.A., Amelung, F., Jonsson, S., 2000. Remote sensing of volcano surface and internal processes using radar interferometry. In: Mouginis-Mark, P.J., Crisp, J.A., Fink, J.H. (Eds.), Remote Sensing of Active Volcanism, Geophysical Monograph, vol. 116. American Geophysical Union, Washington, DC, pp. 179–206.